CLEAN
Soil Air Water

Renewables

Sustainability

Environmental Monitoring

WILEY

Guilin Han[1]
Fushan Li[2]
Yang Tang[2]

[1]School of Scientific Research, China University of Geosciences (Beijing), Beijing, P. R. China

[2]The State Key Laboratory of Environmental Geochemistry, Institute of Geochemistry, Chinese Academy of Sciences, Guiyang, P. R. China

Research Article

Organic Matter Impact on Distribution of Rare Earth Elements in Soil Under Different Land Uses

This study investigated the enrichment and fractionation of rare earth elements (REE) in soils with different soil organic carbon (SOC) concentrations under diverse land uses. The results indicated that there were significant and important differences in soil REE behavior. Their fractionation was strongly and negatively correlated to the middle REE (MREE) and SOC implying that soil organic matter (SOM) acts as the host phase for the REE. Higher total REE concentrations in sites dominated by C4 plants than those dominated by C3 plants, and the significant negative correlation between δ^{13}C and MREE indicated that the organic functional groups that adsorb REE change with the stable isotope composition of SOC. This observation demonstrates the potential use of REE for tracing natural influences on behavior of SOC in the profiles of SOC-rich soils.

1 Introduction

Rare earth elements (REE) are a chemically similar group of elements that have been used extensively to trace geochemical processes in natural systems [1–3]. The redistribution of REE in the products of chemical weathering has been the subject of attention for several decades [4, 5], which, in recent years, has shifted to tracing metal speciation, binding to naturally occurring colloids including organic matter (OM), and their transfer in different environments [6, 7]. Although, REE may accumulate on particulate matter or on nano-colloids of some specific sizes [7–9], the process may lead to fractionation of specific elements in the particulate phases. Such fractionation of REE has been observed within specific soil horizons [10, 11] and in carbonate-dominated areas [12]. Under more alkaline conditions (pH >6), naturally occurring nano-colloids have a strong binding capacity for REE [13, 14].

Weathering and leaching sequences are partly controlled by soil microorganisms and partly by the production, dissolution, movement, and precipitation of organic compounds [15]. Several microorganisms have a high capacity for biosorption of REE ions such as Gd^{3+} [16]. Other explanations for greater release of such metals include metal siderophore complexation at the mineral surface and

subsequent release into soil solution or cell uptake [16]. Moreover, on a nanoscale, the chemical mixture of soil organic matter (SOM) is spatially distinct. In subsoil horizons, physical protection of occluded particulate organic matter (oPOM) was identified as an important mechanism for the stabilization of oPOM [17]. The importance of mineral interaction in the stabilization of subsoil OM is supported by the observation that the radio carbon activity of SOM in subsoil horizons is related to the carbon soluble in hydrofluoric acid in both temperate [18] and tropical [19] soils. Organic matter has recently been shown to be one of the key factors that control REE speciation in aquatic environments such as shallow groundwater, surface water, and soil solutions [20]. This fundamental role has been studied directly, using techniques such as ultrafiltration and electrochemical measurements of organic-rich water [21], as well as indirectly, using models [22].

Karst ecosystems constitute highly fragile environments that have been progressively degraded because of human activities in many regions across the world [23]. In karst regions of Southwest China, the ecological degradation has resulted in many ecological problems including desertification, which is referred to as karst rocky desertification (KRD, [24]). Locally, high permeability at shallow depths in mature karst regions leads to an ecosystem associated with a soilless and water-scarce surface environment [25]. Depending on the storage of REE and SOM in soil, competition for them may lead to the redistribution of REE in soil profile, and the differences in land use and land cover of a given region provide an environmental gradient of soil organic carbon (SOC) content to examine the movement of REE along the soil profile. However, changes in the composition of REE in modern soils at different depths and under different land uses have received little attention so far. The nature of vegetation (forest, grass, crops) affects the weathering of the underlying soil and changes the properties of SOM. Therefore, the

Correspondence: Prof. Guilin Han, School of Scientific Research, China University of Geosciences (Beijing), Beijing 100083, P. R. China
E-mail: hanguilin@cugb.edu.cn

Abbreviations: CQC, grassland; **DJS**, secondary forest; **EF**, enrichment factor; **HREE**, heavy REE; **KRD**, karst rocky desertification; **LREE**, light REE; **MREE**, middle REE; **OM**, organic matter; **oPOM**, occluded particulate organic matter; **PAAS**, post-Archaean Australian shale; **PDB**, Pee Dee Belemnite; **PFA**, perfluoroalkoxy; **REE**, rare earth elements; **SOC**, soil organic carbon; **SOM**, soil organic matter; **YMD**, farmland; **YPG**, shrub land; **ZJT**, virgin forest.

present study aimed to characterize the REE fractions in the total soil volume as well as their distribution at different depths and also to examine the influence of SOM on the migration of REE with a view to obtain some fundamental information for devising suitable measures to protect the fragile soil resources and to improve the land use policies in Puding county, Southwest China.

2 Materials and methods

2.1 Study area

The study site was part of Puding county, which lies in the western part of Guizhou province (26°15.079′–26°16.238′N, 105°46.201–105° 47.038′E) and in Southwest China (Fig. 1). The site has the warm and humid climate typical of the subtropical monsoon climate zone. The mean annual precipitation is approximately 1400 mm, most of which is received between May and October [26]. The mean daily humidity is 79%, and the mean annual temperature is 15.1°C. Puding is dominated by Permian and Triassic carbonate rocks in 1042–1846 m above the sea level. These rocks are usually exposed on the surface, and the soils are thin and discontinuous, resulting in highly fragile environments. Karst rock desertification areas cover 21.5% of Puding county.

The small watershed in the region is a typical karst peak cluster, a depression surrounded on three sides by mountains. The average slope is ≥30°. The five types of land cover at the study site, namely primary or virgin forest (ZJT), secondary forest (DJS), shrub land (YPG), grassland (CQC), and farmland (YMD), represented a range of environments (Tab. 1). The sampling strategy was designed to collect representative data from various land forms, land-use types, and areas with different conversion histories to cover a range of soil conditions. The sampling areas were selected based on field surveys and interviews with farmers and local experts. The vegetation in the grassland and the shrub land, which had been converted to their respective land use in recent decades, was a mix of C4 and C3 plants; the secondary forest land and the virgin forest land were dominated by C3 plants; and the farmland was under maize, a C4 plant and an important food crop.

2.2 Sampling and analysis

One pit was dug in September 2012 (autumn) in each of the sites that represented the five vegetation types (Fig. 1) at Chenqi, a small enclosed karst catchment. Two soil profiles were sampled in the forest lands, one each in ZJT and DJS; the latter is covered with broad-leaved deciduous trees with no understory left and a canopy cover of about 80%, a result of reforestation initiated 30 years after clearing the original forest. Two more soil profiles were sampled, one each in YPG and CQC, both of which had been forests and were cleared about 30 years ago to raise grain crops and are currently covered with a mix of herbaceous and woody vegetation. The four soil profiles were located on slopes of 30–40° at an elevation of about 1400 m. The soil profile for YMD, covered with maize, was located on a small piece of flat land surrounded by hills. At each site, soil samples were collected at depth intervals of 10 cm up to the boundary between the soil and the underlying rock (Tab. 1). A total of 46 soil samples were collected.

The soil samples were ground thoroughly, in an agate mortar, fine enough to pass through a 75 μm sieve. The powdered samples were then dried in an oven at 105°C for 3 h before being digested as follows [27, 28]: 100 mg of powdered samples were placed in molded

perfluoroalkoxy (PFA) sample jars (Savillex, USA), each filled with 3 mL nitric acid and 1 mL hydrofluoric acid. The jars were heated on a hot plate at 140°C for 7 days to promote further break down of the silicate, fluoride, and carbon compounds. The samples were re-dissolved in 3 mL nitric acid and 1 mL hydrofluoric acid until the solution became clear, indicating complete digestion. To break down the fluorine compounds, 2 mL nitric acid (1:1) was added to the clear solution two times, following which the samples were dried and vaporized on a hot plate. Finally, the digested residue was dissolved in 2% HNO_3 in 100 mL volumetric flasks. The digestion experiment was carried out in the Ultra-Clean Laboratory of the Institute of Geochemistry, Chinese Academy of Sciences. The concentrations of REE in the digested solutions were determined using spectrometry (Agilent 7500a ICP-MS, USA) at the State Key Laboratory of Ore Deposit Geochemistry, Chinese Academy of Sciences.

After removal of carbonates by 6 M HCl, the organic carbon content of the samples was determined by combustion using an elemental analyzer (PE2400, PerkinElmer, USA) with a precision of ≤0.1%. For the analysis of stable isotopes, a sample mass yielding 0.5 mg of carbon was placed in a quartz tube with CuO and a platinum wire, and the sample tube was evacuated and flame-sealed. Organic carbon in the sample was oxidized to CO_2 at 850°C for 5 h; CO_2 was collected and purified cryogenically in a vacuum extraction line; and the quantity of CO_2 was measured before collecting it in the break-seal tube for subsequent mass spectrometric analysis [29]. The ratios of stable isotopes of carbon ($^{13}C/^{12}C$) were measured by MS (MAT-252, Finnigan MAT, USA) at the State Key Laboratory of Environmental Geochemistry, Chinese Academy of Sciences. The contents of organic carbon were expressed as a percentage of dry weight, and the ratio as $\delta^{13}C$ with respect to Pee Dee Belemnite (PDB) standard using the conventional $\delta^{13}C$ notation, as follows:

$$\delta^{13}C\ (\permil) = [(R_{sample}/R_{standard}) - 1] \times 1000 \qquad (1)$$

where R_{sample} and $R_{standard}$ are the $^{13}C/^{12}C$ ratios of the sample and the standard, respectively. The analytical precision was $\delta^{13}C \pm 0.2\permil$.

2.3 Data treatment

Since REE concentrations are naturally variable, the variation in REE composition between samples was assessed using the convention of concentrations normalized to post-Archaean Australian shale (PAAS). Although, it is preferable to normalize data against a reference specific to the study system, such information is often unavailable. In the absence of a system specific reference, PAAS is widely used for normalizing REE concentrations [30]. Chondrite is used in studying endogenous processes, whereas "shales" are applied to study hypergene processes and are commonly used in environmental studies.

Rare earth elements can be divided into heavy REE (HREE), and light REE (LREE) and, at times, a poorly defined group of MREE is also added, depending on their atomic mass and radius [10]: LREE comprises La, Ce, Pr, Pm, Sm, and Eu; HREE comprises Gd, Tb, Dy, Ho, Er, Th, Yb, and Lu; and in the present study, MREE comprising Eu, Gd, Tb, and Dy was also included.

Due to their special electron configuration in the outer shell, Ce and Eu occur as Ce^{4+} and Eu^{2+}; the Eu anomaly, that is its deviation from the neighboring elements, is the petrogenesis of rocks in the drainage basin, and that of Ce is due to Ce (III) being oxidized to Ce (IV) during weathering. The two anomalies (Ce and Eu) [31–33] are
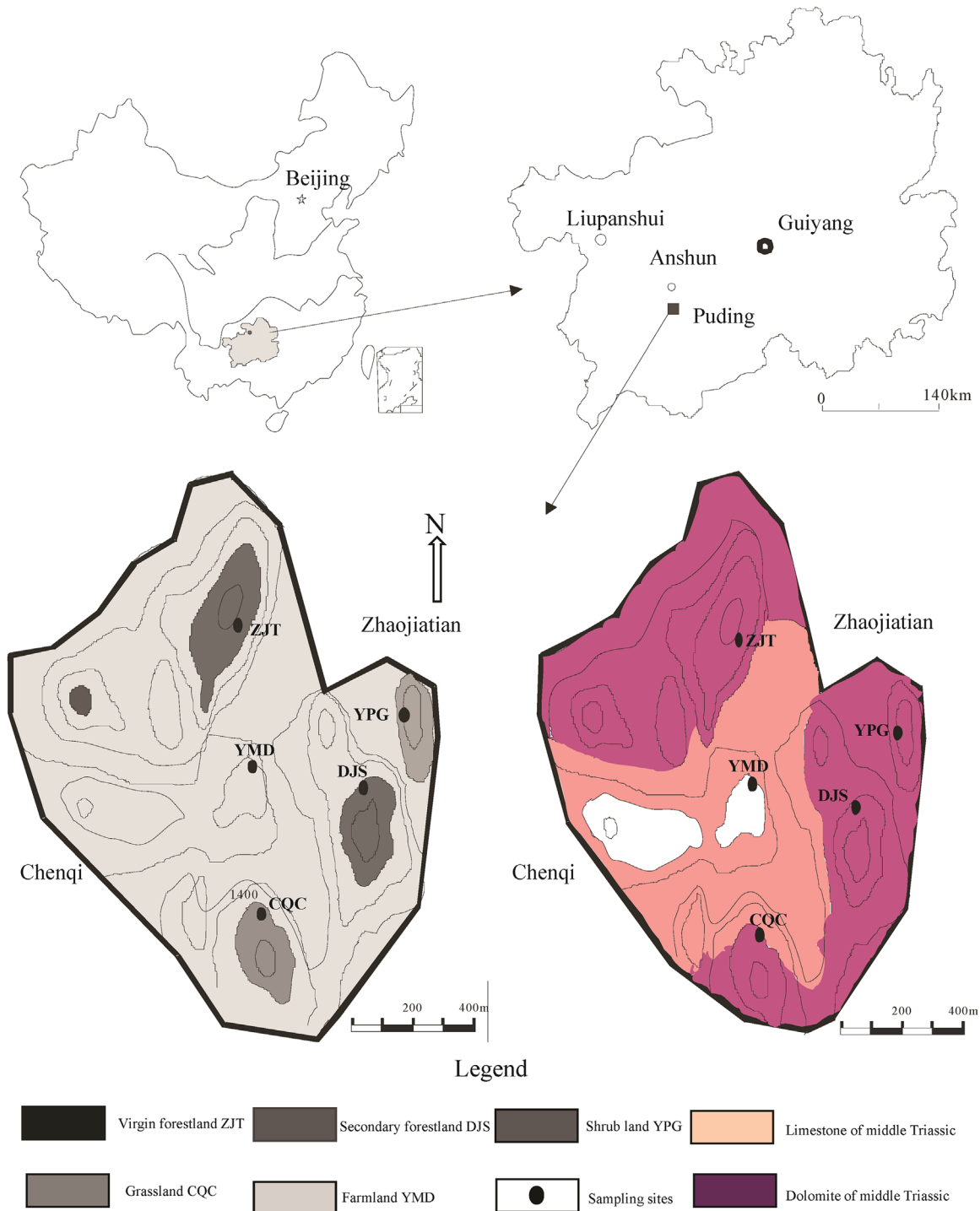
Figure 1. The distribution of various land-use types in the sampling sites in Guizhou province, Southwest China.

defined as follows:

$$Ce\ anomaly = 2\ (Ce/Ce^*)/(La/La^* + Pr/Pr^*) \qquad (2)$$

$$Eu\ anomaly = 2\ (Eu/Eu^*)/(Sm/Sm^* + Gd/Gd^*) \qquad (3)$$

where Ce^*, La^*, Pr^*, Eu^*, Sm^*, and Gd^* represent the concentrations of the respective REE in the PAAS. The Ce anomaly and

the Eu anomaly represent the deviation of Ce and Eu concentrations from those expected from a linear interpolation of the concentrations of La and Pr and of Sm and Gd, respectively, in the PAAS-normalized REE patterns of the samples. It is easy to distinguish the deviation (fractionation) of Ce and Eu from the expected (trivalent) REE. The negative or positive Ce (Eu) anomalies are defined as values of <1 or >1, respectively.

Table 1. Basic characteristics of the five soil profiles in Guizhou province, Southwest China

Land type	Elevation (m)	Latitude	Longitude	Depth (cm)	Dominant vegetation	Visible characteristics
ZJT	1451	N 26°16.238′	E 105°47.038′	0∼55	*Cyclobalanopsis*	0–30 cm: Black, humus layer, no roots
					Cinnamomum camphora (C4)	30–55 cm: Yellow, clayey
DJS	1395	N 26°15.698′	E 105°46.201′	0∼65	*Platycarya longipes* Wu (C4)	0–20 cm: Black, humus layer, no roots
						30–65 cm: Yellow brown, fine grained, rotten roots
YPG	1401	N 26°15.079′	E 105°46.582′	0∼95	*Pyracantha fortuneana* (C3)	0–30 cm: Black, humus layer, abundant plant roots
					Cinnamomum camphora (C4)	30–95 cm: Yellow, moist, clay layer
CQC	1471	N 26°15.641′	E 105°46.433′	0∼85	*Miscanthus floridulus* (C3)	0–30 cm: Black, humus layer, abundant plant roots
						30–85 cm: Yellow limestone soil
YMD	1332	N 26°15.901′	E 105°46.422′	0∼85	Oilseed rape (C3)	0–30 cm: Black, humus layer, tight, no rootlets
					Maize(C4)	30 to 8 to 5 cm: Brown to yellow soil

The assessment of REE concentrations in the weathered carbonate samples from the profiles was carried out by the enrichment factor (EF) [15]:

$$EF_{Zr} = (X/Zr)_i / (X/Zr)_b$$

where X is the REE, Zr is a reference element in the sample, i represents the soil depth, and b represents the bottom of the soil. If $EF = 1$, the REE were at the background level; if $EF \geq 1$, the REE were probably enriched; and if $EF \leq 1$, the REE were depleted.

3 Results and discussion

3.1 Concentration of rare earth elements

Total REE concentrations (ΣREE) exceeded 117 mg/kg (except in the surface and subsurface soil in YPG and in the sample taken from a depth of −15 cm in DJS) in all horizons of all the five profiles, with a maximum value (296.51 mg/kg) in the bottom soil in YMD (Supporting Information Tab. S1). Total REE concentrations in YMD were distinctly different from those in the other four profiles, and soils in YPG were characterized by relatively low total REE concentrations, particularly at the surface (34.6 mg/kg, Supporting
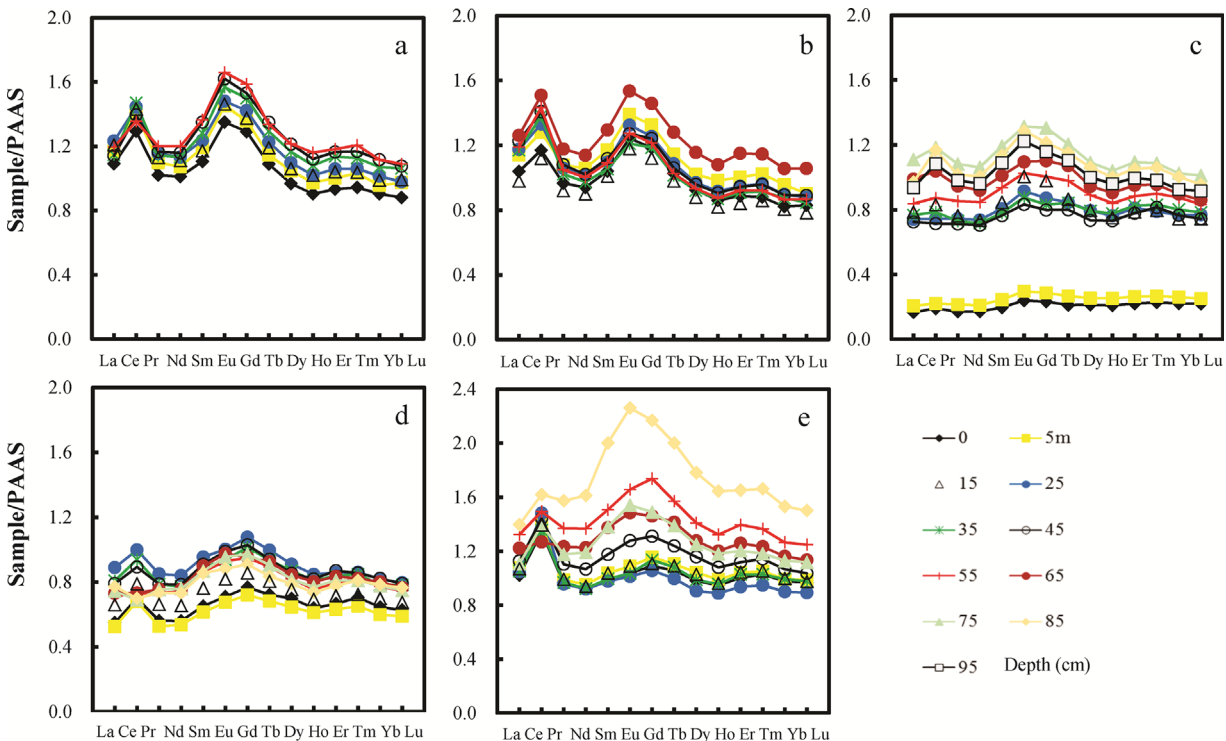

Figure 2. Fractionation patterns of rare earth elements (PAAS normalized) in soil profiles from the five land uses studied in Guizhou province, Southwest China. (a) Virgin forest land (ZJT), (b) secondary forest land (DJS), (c) shrub land (YPG), (d) grassland (CQC), and (e) farmland (YMD).

Information Tab. S1). Total REE concentrations in the surface samples from ZJT and DJS were 213.9 and 197.5 mg/kg, respectively. Changes in the total REE concentration with depth varied within a narrow range in each of the five soil profiles; in general, total REE concentrations increased with depth, becoming more or less stable in the deepest layers. However, the rate of increase was different for each profile, being the highest in YMD.

3.2 Fractionation of rare earth elements

PAAS-normalized REE fractionation patterns are shown in Fig. 2 and Supporting Information Tab. S1 for all the soil samples. It is clear that the pattern is far from flat. MREE enrichment was a dominant feature of the fractionation patterns, more pronounced in samples from the upper layers. In addition, a slight relative depletion in HREE was also apparent in many of the samples, except a few including that in the surface soil in YPG. The extent of variation in REE fractionation patterns did not increase with depth.

A consistently positive Ce anomaly (Ce anomaly values ≥ 1.2) was seen in most soil samples (Fig. 2), a pattern that can be explained by redox chemistry: Ce is controlled by redox equilibrium between

dissolved Ce^{3+} species and dissolved Ce^{4+} species; Ce forms Ce oxide hydrate, which is retained in the surface layer in hot and humid environments such as that in Puding catchment but migrates to the deeper layers during weathering, thereby enriching Ce in the soil. The depletion of Eu, on the other hand, is generally inherited from the bedrock and not as a result of surficial processes [34]. Therefore, Eu did not show any significantly positive anomaly (the value in most samples was about 1) because Eu^{2+} released during weathering; is oxidized to Eu^{3+} and behaves like any other trivalent REE [35].

3.3 Soil organic carbon

Concentrations of SOC generally decreased with depth, as can be seen in Supporting Information Tab. S1, as was also observed in an earlier study [36]. The carbon content ranged from 7.92 to 0.48%. Such a pattern appears to have become a characteristic feature of soils in Guizhou province, which have been investigated by Han et al. [37]. SOC in YPG (shrub land) and CQC (grassland) was significantly higher and decreased more significantly with depth than that in ZJT and DJS (forest lands) and YMD (farmland) because of the greater productivity and inputs from the C4 plants. The lowest
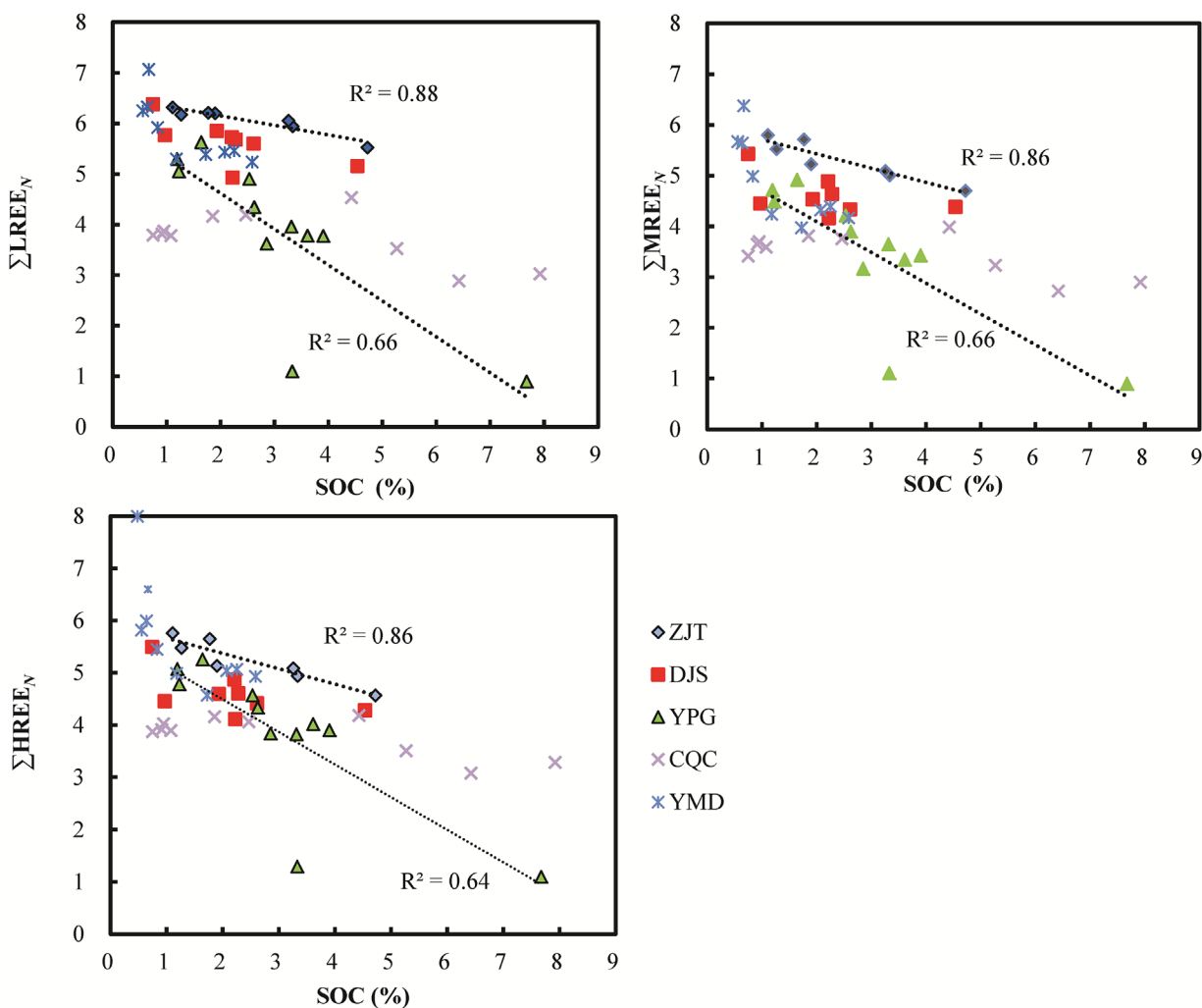

Figure 3. Relationships between soil organic carbon contents and $\sum LREE_N$, $\sum MREE_N$, and $\sum HREE_N$ in soils with different land uses in Guizhou province, Southwestern China.

concentrations of SOC were recorded in YMD because maize was grown on the land.

3.4 Soil organic carbon and PAAS-normalized patterns

As can be seen in Fig. 3, REE_N (PAAS-normalized patterns) decreased as the content of SOC increased. The relationship of LREE, MREE, and HREE with SOC contents also showed a similar pattern; SOC content was strongly correlated to $LREE_N$ ($R^2 = 0.88$, $p < 0.001$), $MREE_N$ ($R^2 = 0.86$, $p < 0.001$), and $HREE_N$ ($R^2 = 0.86$, $p < 0.001$) in forest land, indicating that SOC plays a major role in determining the level of REE combined forms in soil. The correlations were fairly close in grassland as well: $LREE_N$ ($R^2 = 0.66$, $p < 0.001$), $MREE_N$ ($R^2 = 0.66$, $p < 0.001$), and $HREE_N$ ($R^2 = 0.64$, $p < 0.001$). However, the correlations were not significant in the case of other land uses (shrub land and farmland). The importance of OM in mobilizing trace metals is well recognized [21, 38–40] and reported in various climatic regions [21, 41]. The dynamics of REE in different organic-rich soils under different land uses are poorly investigated, despite the extensive use of REE concentrations and their respective fractionation patterns in tracing geochemical processes, and assessing the influence of anthropogenic activity on natural systems [42]. The results demonstrate that REEs in the systems studied can be readily distinguished on the basis of land use; soils rich in OM, such as those from shrub land and farmland, have a lower capacity for adsorption of REE than other soils.

Organic matter was abundant in YPG and CQC. The influence of natural OM on the retention and fractionation of REE was examined by Pourret et al. [22], who reported that REE formed strongly bound complexes with humic substances at near-neutral pH values. Therefore, it is likely that adsorption of REE on humus in the solid phase influenced REE behavior in the organic-rich soils used in the present study and explains the high total REE content.

3.5 Factors affecting enrichment of rare earth elements and δ13C of soils

In the present study, $\delta^{13}C$ values of SOC ranged from -25.5 to $-17.0\permil$. In the upper layer (30 cm), $\delta^{13}C$ values were higher than those in the deeper layers: The values decreased with depth (Supporting Information Tab. S1 and Fig. 4). The fractionation patterns of the REE showed a similar trend. The patterns of $\delta^{13}C$ values in all the five profiles reflect the input from vegetation at each site. For example, the $\delta^{13}C$ values of the forested sites (ZJT and DJS) reflect the typical predominance of C3 plants, whereas those in the shrub land (YPG), grassland (CQC), and cropland (YMD) reflect the typical predominance of C4 plants.

The evolution of REE enrichment factors (EF_{Zr}) with soil depth is shown in Tab. 2 and Fig. 4: $\delta^{13}C_{SOC}$ values were higher near the surface, down to 30 cm depth, as discussed above. MREE and HREE in shrub land site (YPG) showed higher REE enrichment at 30 cm depth but were markedly depleted in farmland site (YMD). The forest land
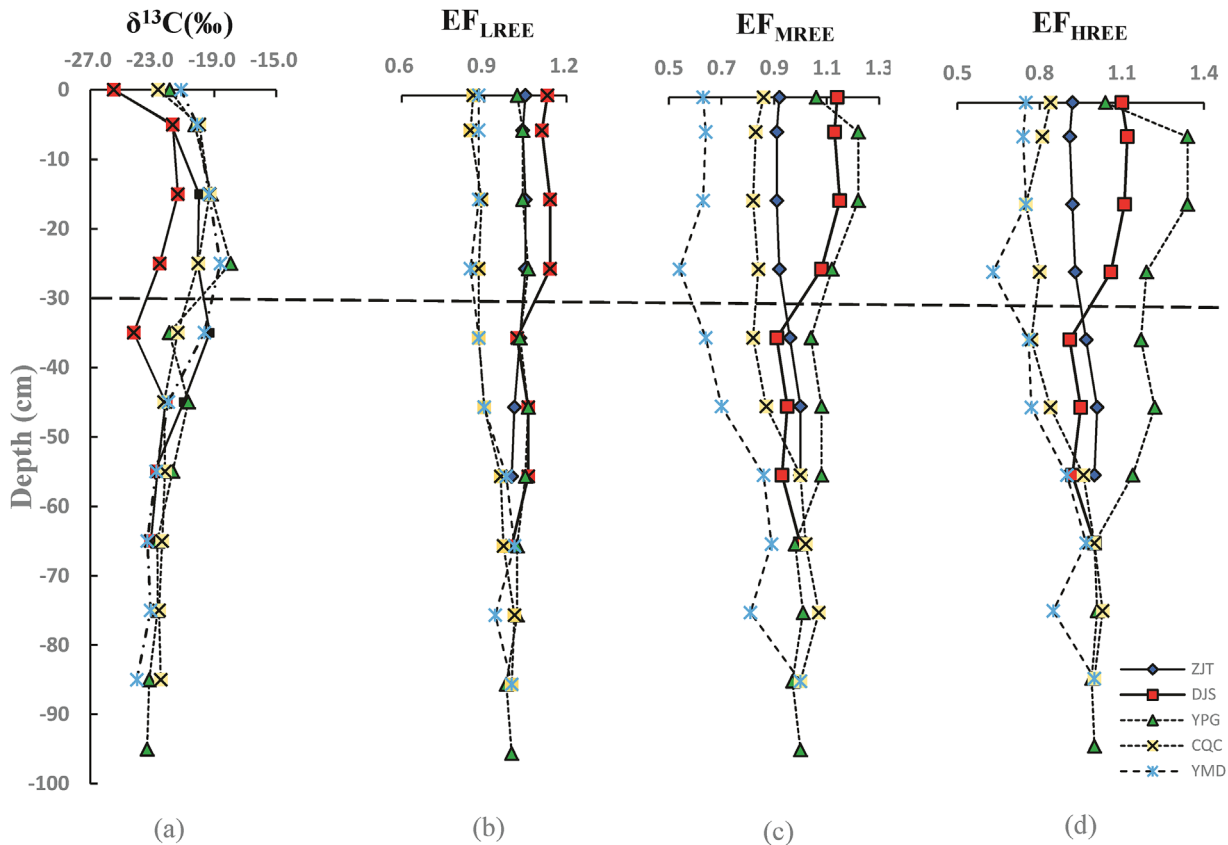

Figure 4. Evolution of organic carbon within soil profiles (a), and variation in enrichment factors for LREE (b), MREE (c), and HREE (d) with depth under different land uses in Guizhou province, Southwestern China.

Table 2. Enrichment factors (EF: normalized to Zr of the bottom soil from each profile) obtained for REE in samples from five soil profiles at Puding in Guizhou province, Southwest China

Land use	Depth	EF_{HREE}	EF_{MREE}	EF_{LREE}	Zr (mg/kg)
ZJT	0	1.05	0.92	0.92	157.0
	−5	1.04	0.91	0.91	170.0
	−15	1.05	0.91	0.92	173.0
	−25	1.05	0.92	0.93	175.0
	−35	1.03	0.96	0.97	178.0
	−45	1.01	1.00	1.01	177.0
	−55	1.00	1.00	1.00	180.0
DJS	0	1.13	1.14	1.10	147.0
	−5	1.11	1.13	1.12	165.0
	−15	1.14	1.15	1.11	69.0
	−25	1.14	1.08	1.06	164.0
	−35	1.02	0.91	0.91	184.0
	−45	1.06	0.95	0.95	183.0
	−55	1.06	0.93	0.92	183.0
	−65	1.00	1.00	1.00	208.0
YPG	0	1.02	1.06	1.04	15.1
	−5	1.04	1.22	1.34	17.6
	−15	1.04	1.22	1.34	66.2
	−25	1.06	1.12	1.19	59.3
	−35	1.03	1.04	1.17	62.6
	−45	1.06	1.08	1.22	56.9
	−55	1.05	1.08	1.14	69.5
	−65	1.02	0.98	1.00	82.7
	−75	1.02	1.01	1.01	94.3
	−85	0.98	0.97	0.99	93.1
	−95	1.00	1.00	1.00	86.2
CQC	0	0.86	0.86	0.84	55.8
	−5	0.85	0.83	0.81	54.2
	−15	0.89	0.82	0.75	79.5
	−25	0.88	0.84	0.80	62.8
	−35	0.88	0.82	0.77	74.7
	−45	0.90	0.87	0.84	71.1
	−55	0.96	1.00	0.96	58.0
	−65	0.97	1.02	1.00	58.0
	−75	1.01	1.07	1.03	54.0
	−85	1.00	1.00	1.00	55.0
YMD	0	0.88	0.63	0.75	107.0
	−5	0.88	0.64	0.74	112.0
	−15	0.88	0.63	0.75	111.0
	−25	0.85	0.54	0.63	118.0
	−35	0.88	0.64	0.76	108.0
	−45	0.90	0.70	0.77	115.0
	−55	0.98	0.86	0.90	119.0
	−65	1.01	0.89	0.97	101.0
	−75	0.94	0.81	0.85	111.0
	−85	1.00	1.00	1.00	129.0

$EF = (X_i/Zr_i)/(X_b/Zr_b)$, X represents the layer of soil, i represents the depth of soil, b represents the bottom of soil.

and grassland sites showed slightly higher values of REE (HREE and MREE) in the upper horizons and the values remained fairly constant with depth, whereas EF_{LREE} values showed no variation across the different land uses. Organic matter is the most important reductant as a result of its decomposition by oxygen, which is closely associated with OM [43]. The present study confirmed that the great diversity of organic compounds produced by the decomposition of plant litter of different species greatly influences the behavior of REE in soils, as was observed elsewhere [44]. Soil organic matter has many negatively charged groups per unit dry weight and, consequently, a high capacity to adsorb or chelate divalent and trivalent cations [45]. The organic compounds originating from different vegetation types

decomposed to form various functional groups to adsorb REE accompanying the signals from stable isotope compositions of SOC (Fig. 4).

Weathering and leaching sequences are partly controlled by soil microorganisms and partly by the production, dissolution, movement, and precipitation of organic compounds. Thus, the patterns of REE fractionation in the soil profiles examined in the present study point to the influence of OM on REE retention. The marked enrichment in the study was consistent across all environments for total digests. Recent research indicates that MREE enrichment can be due to the preferential complexation of MREE with natural OM, compared to the weaker complexation of both LREE and HREE [46]. Taking into account the fact that the experimental soils were rich in OM, the observed MREE enrichment is consistent with REE complexation by OM.

The strong negative correlation between the magnitude of the MREE enrichment and $\delta^{13}C_{SOC}$ values suggests that a common soil fraction influences the enrichment of both MREE and HREE relative to LREE. In alkaline environments, the stability constant for REE-organic complexes is the highest for MREE, followed, in that order, by HREE, and LREE-organic complexes [30, 46].

REE can also be absorbed onto clay minerals such as kaolinite, smectite, and chlorite under neutral pH [47–49] and released from the surface of these minerals under acidic conditions [50]. In addition, in soils rich in OM, humic substances can coat clay minerals, and REE sorption is thus influenced more by the interaction with this surface layer of humus, than with the surface of the underlying clay particles [51]. This observation suggests that although soil minerals, especially clay minerals, may have had some influence on REE retention in the present experiment, it is more likely that the influence was negligible, whereas that of the OM was substantial. The different patterns of REE enrichment in grassland seen in the soil profile may be explained by the difference in the storage of REE between OM and clay minerals. In comparing REE enrichment in soils under different land uses, the difference between the surface down to 30 cm depth and the deeper layer may be due to the distribution of both OM and the clay mineral assemblies.

4 Concluding remarks

Research on the retention and fractionation of REE at different levels of SOM is somewhat scant, particularly that based on fully digested soil samples. The present study showed strong negative correlations between REE and SOC and between EF_{REE} and $\delta^{13}C_{SOC}$, which is consistent with the retention of REE in soil. The detailed study involving five types of land use made it possible to distinguish between different patterns of REE mobilization under different land uses and showed that REE enrichment and fractionation trends varied across a gradient of SOC concentration. Soils rich in organic carbon displayed a greater enrichment of total REE than other soils, and the studied sites displayed a significantly negative correlation between values of $\delta^{13}C_{SOC}$ and the magnitude of MREE enrichment.

CLEAN
Soil Air Water

References

[1] M. Åström, Abundance and Fractionation Patterns of Rare Earth Elements in Streams Affected by Acid Sulphate Soils, *Chem. Geol.* **2001**, *175* (3), 249–258.

[2] S. A. Welch, A. G. Christy, L. Isaacson, D. Kirste, Mineralogical Control of Rare Earth Elements in Acid Sulfate Soils, *Geochim. Cosmochim. Acta* **2009**, *73* (1), 44–64.

[3] C. Wang, Y. Liang, W. Xu, On the Significance of Temperatures Derived From Major Element and REE Based Two-Pyroxene Thermometers for Mantle Xenoliths From the North China Craton, *Lithos* **2015**, *224*, 101–113.

[4] I. Hill, R. Worden, I. Meighan, Yttrium: The Immobility-Mobility Transition During Basaltic Weathering, *Geology* **2000**, *28* (10), 923–926.

[5] L. C. Patino, M. A. Velbel, J. R. Price, J. A. Wade, Trace Element Mobility During Spheroidal Weathering of Basalts and Andesites in Hawaii and Guatemala, *Chem. Geol.* **2003**, *202* (3), 343–364.

[6] J. P. Gustafsson, E. Dässman, M. Bäckström, Towards a Consistent Geochemical Model for Prediction of Uranium (VI) Removal From Groundwater by Ferrihydrite, *Appl. Geochem.* **2009**, *24* (3), 454–462.

[7] X. Zhu, F. Yang, C. Wei, T. Liang, Bioaccessibility of Heavy Metals in Soils Cannot Be Predicted by a Single Model in Two Adjacent Areas, *Environ. Geochem. Health* **2016**, *38* (1), 233–241.

[8] D. Moraetis, F. Stamati, M. Kotronakis, T. Fragia, N. Paranychnianakis, N. P. Nikolaidis, Identification of Hydrologic and Geochemical Pathways Using High Frequency Sampling, REE Aqueous Sampling and Soil Characterization at Koiliaris Critical Zone Observatory, Crete, *Appl. Geochem.* **2011**, *26*, S101–S104.

[9] E. Neubauer, S. J. Köhler, F. von der Kammer, H. Laudon, T. Hofmann, Effect of pH and Stream Order on Iron and Arsenic Speciation in Boreal Catchments, *Environ. Sci. Technol.* **2013**, *47* (13), 7120–7128.

[10] G. Tyler, Vertical Distribution of Major, Minor, and Rare Elements in a Haplic Podzol, *Geoderma* **2004**, *119* (3), 277–290.

[11] P. Stille, M. Steinmann, M.-C. Pierret, F. Gauthier-Lafaye, F. Chabaux, D. Viville, L. Pourcelot, et al., The Impact of Vegetation on REE Fractionation in Stream Waters of a Small Forested Catchment (the Strengbach Case), *Geochim. Cosmochim. Acta* **2006**, *70* (13), 3217–3230.

[12] K. H. Johannesson, I. M. Farnham, C. Guo, K. J. Stetzenbach, Rare Earth Element Fractionation and Concentration Variations Along a Groundwater Flow Path Within a Shallow, Basin-Fill Aquifer, Southern Nevada, USA, *Geochim. Cosmochim. Acta* **1999**, *63* (18), 2697–2708.

[13] K. A. Quinn, R. H. Byrne, J. Schijf, Sorption of Yttrium and Rare Earth Elements by Amorphous Ferric Hydroxide: Influence of pH and Ionic Strength, *Mar. Chem.* **2006**, *99* (1), 128–150.

[14] R. Marsac, M. Davranche, G. Gruau, A. Dia, M. Pédrot, M. Le Coz-Bouhnik, N. Briant, Effects of Fe Competition on REE Binding to Humic Acid: Origin of REE Pattern Variability in Organic Waters, *Chem. Geol.* **2013**, *342*, 119–127.

[15] J. Peng, R. Hu, L. Qi, J. Zhao, Y. Fu, REE Distribution Pattern for the Hydrothermal Calcites From the Xikuangshan Antimony Deposit and Its Constraining Factors, *Geol. Rev.* **2004**, *50* (1), 25–32.

[16] Y. Andres, G. Thouand, M. Boualam, M. Mergeay, Factors Influencing the Biosorption of Gadolinium by Micro-Organisms and Its Mobilisation From Sand, *Appl. Microbiol. Biotechnol.* **2000**, *54* (2), 262–267.

[17] K. Eusterhues, C. Rumpel, I. Kögel-Knabner, Composition and Radiocarbon Age of HF-Resistant Soil Organic Matter in a Podzol and a Cambisol, *Org. Geochem.* **2007**, *38* (8), 1356–1372.

[18] S. Spielvogel, J. Prietzel, I. Kögel-Knabner, Soil Organic Matter Stabilization in Acidic Forest Soils Is Preferential and Soil Type-Specific, *Eur. J. Soil Sci.* **2008**, *59* (4), 674–692.

[19] C. Rumpel, V. Chaplot, A. Chabbi, C. Largeau, C. Valentin, Stabilisation of HF Soluble and HCl Resistant Organic Matter in Sloping Tropical Soils Under Slash and Burn Agriculture, *Geoderma* **2008**, *145* (3), 347–354.

[20] A. Dia, G. Gruau, G. Olivié-Lauquet, C. Riou, J. Molénat, P. Curmi, The Distribution of Rare Earth Elements in Groundwaters: Assessing the Role of Source-Rock Composition, Redox Changes and Colloidal Particles, *Geochim. Cosmochim. Acta* **2000**, *64* (24), 4131–4151.

[21] J. Ingri, A. Widerlund, M. Land, Ö. Gustafsson, P. Andersson, B. Öhlander, Temporal Variations in the Fractionation of the Rare Earth Elements in a Boreal River; the Role of Colloidal Particles, *Chem. Geol.* **2000**, *166* (1), 23–45.

[22] O. Pourret, M. Davranche, G. Gruau, A. Dia, New Insights Into Cerium Anomalies in Organic-Rich Alkaline Waters, *Chem. Geol.* **2008**, *251* (1), 120–127.

[23] M. Parise, J. De Waele, F. Gutierrez, Current Perspectives on the Environmental Impacts and Hazards in Karst, *Environ. Geol.* **2009**, *58* (2), 235–237.

[24] H. Ding, Y.-C. Lang, C.-Q. Liu, The Impact of Land Use and Land Cover Changes on Solute Dynamics in Seepage Water of Soil From Karst Hillslopes of Southwest China, *Appl. Geochem.* **2011**, *26*, S183–S186.

[25] H. LeGrand, Hydrological and Ecological Problems of Karst Regions, *Science* **1973**, *179* (4076), 859–864.

[26] M. Zhao, C. Zeng, Z. Liu, S. Wang, Effect of Different Land Use/Land Cover on Karst Hydrogeochemistry: A Paired Catchment Study of Chenqi and Dengzhanhe, Puding, Guizhou, SW China, *J. Hydrol.* **2010**, *388* (1), 121–130.

[27] P. Roy, W. Smykatz-Kloss, REE Geochemistry of the Recent Playa Sediments From the Thar Desert, India: An Implication to Playa Sediment Provenance, *Chem. Erde* **2007**, *67* (1), 55–68.

[28] H.-S. Tang, Y.-J. Chen, M. Santosh, H. Zhong, T. Yang, REE Geochemistry of Carbonates From the Guanmenshan Formation, Liaohe Group, NE Sino-Korean Craton: Implications for Seawater Compositional Change During the Great Oxidation Event, *Precambrian Res.* **2013**, *227*, 316–336.

[29] T. W. Boutton, W. W. Wong, D. L. Hachey, L. S. Lee, M. P. Cabrera, P. D. Klein, Comparison of Quartz and Pyrex Tubes for Combustion of Organic Samples for Stable Carbon Isotope Analysis, *Anal. Chem.* **1983**, *55* (11), 1832–1833.

[30] C. Laveuf, S. Cornu, A Review on the Potentiality of Rare Earth Elements to Trace Pedogenetic Processes, *Geoderma* **2009**, *154* (1), 1–12.

[31] E. R. Sholkovitz, W. M. Landing, B. L. Lewis, Ocean Particle Chemistry: The Fractionation of Rare Earth Elements Between Suspended Particles and Seawater, *Geochim. Cosmochim. Acta* **1994**, *58* (6), 1567–1579.

[32] G. Han, C.-Q. Liu, Dissolved Rare Earth Elements in River Waters Draining Karst Terrains in Guizhou Province, China, *Aquat. Geochem.* **2007**, *13* (1), 95–107.

[33] G. Han, Z. Xu, Y. Tang, G. Zhang, Rare Earth Element Patterns in the Karst Terrains of Guizhou Province, China: Implication for Water/Particle Interaction, *Aquat. Geochem.* **2009**, *15* (4), 457–484.

[34] F. Perri, S. Critelli, A. Martín-Algarra, M. Martín-Martín, V. Perrone, G. Mongelli, M. Zattin, Triassic Redbeds in the Malaguide Complex (Betic Cordillera, Spain): Petrography, Geochemistry and Geodynamic Implications, *Earth Sci. Rev.* **2013**, *117*, 1–28.

[35] S. R. Taylor, S. M. McLennan, *The Continental Crust: Its Composition and Evolution*, Blackwell, Oxford **1985**.

[36] X. Fang, Z. Xue, B. Li, S. An, Soil Organic Carbon Distribution in Relation to Land Use and Its Storage in a Small Watershed of the Loess Plateau, China, *Catena* **2012**, *88* (1), 6–13.

[37] G. Han, F. Li, Y. Tang, Variations in Soil Organic Carbon Contents and Isotopic Compositions Under Different Land Uses in a Typical Karst Area in Southwest China, *Geochem. J.* **2015**, *49* (1), 63–71.

[38] A. Navas, L. Gaspar, L. Quijano, M. López-Vicente, J. Machín, Patterns of Soil Organic Carbon and Nitrogen in Relation to Soil Movement

Under Different Land Uses in Mountain Fields (South Central Pyrenees), *Catena* **2012**, *94*, 43–52.

[39] X. Wei, H. Ji, S. Wang, H. Chu, C. Song, The Formation of Representative Lateritic Weathering Covers in South-Central Guangxi (Southern China), *Catena* **2014**, *118*, 55–72.

[40] Y. Xiong, Organic Species of Lanthanum in Natural Environments: Implications to Mobility of Rare Earth Elements in Low Temperature Environments, *Appl. Geochem.* **2011**, *26* (7), 1130–1137.

[41] W. -F. Tan, R. Zhang, H. Cao, C. -Q. Huang, Q. -K. Yang, M. -K. Wang, L. K. Koopal, Soil Inorganic Carbon Stock Under Different Soil Types and Land Uses on the Loess Plateau Region of China, *Catena* **2014**, *121*, 22–30.

[42] G. Mongelli, M. Paternoster, G. Rizzo, R. Sinisi, Trace Elements and REE Fractionation in Subsoils Developed on Sedimentary and Volcanic Rocks: Case Study of the Mt. Vulture Area, Southern Italy, *Int. J. Earth Sci.* **2014**, *103* (4), 1125–1140.

[43] J. -L. Ma, G. -J. Wei, Y. -G. Xu, W. -G. Long, W. -D. Sun, Mobilization and Re-Distribution of Major and Trace Elements During Extreme Weathering of Basalt in Hainan Island, South China, *Geochim. Cosmochim. Acta* **2007**, *71* (13), 3223–3237.

[44] K. Semhi, S. Chaudhuri, N. Clauer, Fractionation of Rare-Earth Elements in Plants During Experimental Growth in Varied Clay Substrates, *Appl. Geochem.* **2009**, *24* (3), 447–453.

[45] Z. Wu, J. Luo, H. Guo, X. Wang, C. Yang, Adsorption Isotherms of Lanthanum to Soil Constituents and Effects of pH, EDTA and Fulvic Acid on Adsorption of Lanthanum Onto Goethite and Humic Acid, *Chem. Speciation Bioavailability* **2001**, *13* (3), 75–81.

[46] J. Tang, K. H. Johannesson, Ligand Extraction of Rare Earth Elements From Aquifer Sediments: Implications for Rare Earth Element Complexation With Organic Matter in Natural Waters, *Geochim. Cosmochim. Acta* **2010**, *74* (23), 6690–6705.

[47] F. Coppin, G. Berger, A. Bauer, S. Castet, M. Loubet, Sorption of Lanthanides on Smectite and Kaolinite, *Chem. Geol.* **2002**, *182* (1), 57–68.

[48] T. De Putter, L. André, A. Bernard, C. Dupuis, J. Jedwab, D. Nicaise, A. Perruchot, Trace Element (Th, U, Pb, REE) Behaviour in a Cryptokarstic Halloysite and Kaolinite Deposit From Southern Belgium: Importance of "Accessory" Mineral Formation for Radioactive Pollutant Trapping, *Appl. Geochem.* **2002**, *17* (10), 1313–1328.

[49] M. Prudêncio, M. Dias, J. Waerenborgh, F. Ruiz, M. Trindade, M. Abad, R. Marques, et al., Rare Earth and Other Trace and Major Elemental Distribution in a Pedogenic Calcrete Profile (Slimene, NE Tunisia), *Catena* **2011**, *87* (1), 147–156.

[50] R. Cullers, S. Chaudhuri, N. Kilbane, R. Koch, Rare-Earths in Size Fractions and Sedimentary Rocks of Pennsylvanian-Permian Age From the Mid-Continent of the USA, *Geochim. Cosmochim. Acta* **1979**, *43* (8), 1285–1301.

[51] Y. Wan, C. Liu, The Effect of Humic Acid on the Adsorption of REEs on Kaolin, *Colloids Surf., A* **2006**, *290* (1), 112–117.